Materials Research. 2017; 20(4): 912-919
DOI: http://dx.doi.org/10.1590/1980-5373-MR-2016-0684

Easy and Fast Preparation of TiO_2 - based Nanostructures Using Microwave Assisted Hydrothermal Synthesis

***Bruna Andressa Bregadiolli*[a]*, Silvia Leticia Fernandes*[a,b], *Carlos Frederico de Oliveira Graeff*[b,c]**

[a] *POSMAT, Universidade Estadual Paulista "Júlio de Mesquita Filho", Av. Eng. Luiz Edmundo C. Coube 14-01, 17033-360, Bauru, SP, Brazil*
[b] *Instituto de Química de Araraquara, Universidade Estadual Paulista "Júlio de Mesquita Filho" Prof. Francisco Degni 55, 14800-060, Araraquara, SP, Brazil*
[c] *Departamento de Física, Universidade Estadual Paulista "Júlio de Mesquita Filho", Av. Eng. Luiz Edmundo C. Coube 14-01, 17033-360, Bauru, SP, Brazil*

Received: September 17, 2016; Revised: February 22, 2017; Accepted: March 10, 2017

TiO_2 derivatives with distinct morphologies have been successfully obtained by microwave assisted hydrothermal synthesis in acidic and alkaline medium using mild conditions. Titanium tetraisopropoxide (TTIP) was used as precursor in different environmental conditions under low temperatures, inferior to 150 °C, and short synthesis times, from 2 to 60 min. X ray diffraction (XRD), scanning electron microscopy (SEM), transmission electron microscopy (TEM) and N_2 adsorption at 77 K (BET) were used to characterize the microstructural properties of the oxides. In the acidic synthesis the reaction time and temperature are not accompanied by significant changes in the structure of the material. However, in the basic conditions, the concentration of Na^+ ions strongly influences the particle morphology and growth. The morphology of the nanoparticles shows irregular spheres in acidic conditions, while in alkaline medium, needle like structures are formed as well as aggregated nanotube-like structures synthesized in only 30 min. Besides the difference in the morphology and structure, in both systems, high surface area was obtained.

Keywords: *nanostructures, titanium dioxide, microwave assisted hydrothermal synthesis, crystal growth*

1. Introduction

Nanocrystalline titania (TiO_2) has been intensively investigated due to its numerous applications in many fields such as photocatalysis, photovoltaic cells and gas sensors.[1] It is cheap, abundant, chemically stable and a multi-functional material. There are three natural polymorphs of TiO_2: rutile, brookite and anatase. Anatase has a low electron hole recombination rate and due to its high photoactivity is believed to be the most favorable phase for solar energy conversion[2] and photocatalysis.[3] It is an n-type semiconductor with an indirect band gap of 3.2 eV.[4] Particle size has great influence on the structure and properties of TiO_2. In the nanometric regime, anatase is the most stable polymorph.[5] For example in dye sensitized solar cells (DSSC), small particle sizes are desired since greater surface area increases the contact of the nanoparticles with the dye and thus optimizes charge transfer and decreases charge recombination.[6]

For each application, careful tailoring of specific properties such as phase composition, surface area and morphology is requested. So, several TiO_2 nanostructures such as spheres,[5] nanorods[7] and nanotubes[8,9] have been synthesized using different techniques including sol-gel, electrochemical, sonochemical and hydrothermal.[8,10] Hydrothermal synthesis is an environmentally friendly methodology used to synthesize nanostructured materials.[11] The starting material, synthesis conditions and processing can drastically change the final product. For example, Kim et al.,[12] obtained well-defined spherical mesoporous TiO_2 prepared from titanium tetraisopropoxide (TTIP). Kasuga et al.[13] have obtained titanates nanotubes from TiO_2 nanopowder with high concentrations of NaOH. The hydrothermal synthesis is typically done using an autoclave with Teflon liners under controlled temperature and/or pressure in aqueous solutions.[1,2,14,15] Despite its advantages, the synthesis can take several hours to be completed.[16] Microwave assisted approach has been used to synthesize many classes of materials such as oxides and hybrid materials.[17-19] This technique provides uniform distribution of energy inside the sample, better reproducibility and excellent control over experimental parameters.[21] Microwave reactions were found to reduce the hydrothermal synthesis time of TiO_2 by typically 1/3,[16,22-25] and in addition can produce single crystals, with less waste and lower temperatures. TTIP is commonly used in conventional and microwave assisted hydrothermal synthesis of TiO_2 under acid conditions,[1,3,8-10,26] but less in alkaline.[27] Most of the titanate nanotubes synthesis using microwave have TiO_2 nanopowders as precursor, as a consequence, higher temperatures and times are needed.[9,22,23] Wu et al.[24] synthesized multiwall structured titanate nanotubes from powders at high NaOH concentration (8–12 M) for 90 min.

* e-mail: brunabregadiolli@fc.unesp.br

Also, Ou et al.[10] obtained nanotubes with surface area of 256 m^2/g synthesized at 130 °C for 90 min.

In this work, we present an easy and fast route for TiO_2 nanostrucutures synthesis using microwave assisted hydrothermal technique in alkaline and acidic mediums. We demonstrate an environmentally friendly synthesis that uses mild conditions, fast reaction times and low temperatures and gives nanoparticles with different morphologies, high yield and surface area. We have obtained titanate needle like particles after 30 min of synthesis using TTIP in alkaline medium. The facility in producing these nanostructures, its reproducibility and low cost make it attractive for industrial applications.

2. Experimental

Titanium tetraisopropoxide (TTIP) (Alfa-Aesar 97%), HNO_3 (Dinâmica) and NaOH (Synth) were used as received. For the acidic synthesis, 12 mL (0.4 mol) of TTIP was added dropwise in a 0.01 M HNO_3 solution. For the alkalyne synthesis, 12 mL (0.4 mol) of TTIP was added dropwise in NaOH solutions with different concentrations: 0.1, 1 and 10 M. The solution volume used was fixed at 40 mL in a 100 mL autoclave. In both cases, the precursor solution was stirred for 6 h at 80 °C. The solution was poured into a Teflon autoclave placed inside a modified domestic microwave oven (Panasonic Piccolo 800 W) coupled with an external temperature controller (Incon CNT120). The pressure of the system was not externally controlled and reached a maximum of 10 bar. The synthesis temperature varied from 110 to 150 °C and the synthesis time from 2 to 60 min. Subsequent to the synthesis, the colloidal solution was washed with water. Notice that the alkaline synthesis at 10 M (sample HMB150-30-10) was washed with HCl 0.1 M in order to remove the remaining Na^+ ions.[13] The solutions were centrifuged at 2500 rpm and dried in an oven at 60 °C. The samples were named as follow: HM (for the acidic medium) or HMB (for the alkaline medium), followed by the temperature and synthesis time. For the HMB samples, in addition the NaOH concentration is presented. Details about the synthesis parameters used are presented in the Supplementary Material, Table S1. X-ray diffraction (XRD) was done in a Rigaku RINT2000 diffractometer with CuKα radiation, using 40 kV and 20 mA. Scanning electron microscopies (SEM) were performed using a FEI Inspect F50 and a Philips XL30-FEG. The size of the nanoparticles was measured using transmission electron microscopy (TEM) using a Philips CM120 and 200 kV. The surface area and pore size were determined by Brunauer–Emmett–Teller ($_{BET}$) adsorption of nitrogen at 77K in a Micromeritics ASAP 2010. The surface area was calculated from the adsorption isotherm.

3. Results and discussion

3.1 Acidic medium

Table S1 summarizes the results of the acidic medium synthesis as the morphology and the yield for all times and temperatures used. The temperatures were chosen above the boiling point of water to reach the solvent vapor pressure saturation.

Figure 1 shows the XRD pattern of a sample synthetized at 110 °C for 5 min. The patterns exhibits the predominance of the anatase phase (JCPDS 21-1272). However, a diffraction at 2θ = 31.8 ° (* in the Figure 1) attributed to the (211) plane of the brookite phase (JCPDS 29-1360) is observed. It is known that brookite phase can be formed in hydrothermal synthesis in high temperatures and pressure.[28] Also a peak of rutile phase can be observed (# in the Figure 1).[29] The diffractions patterns for all HM samples are similar, see Supplementary Material, Figure S1.

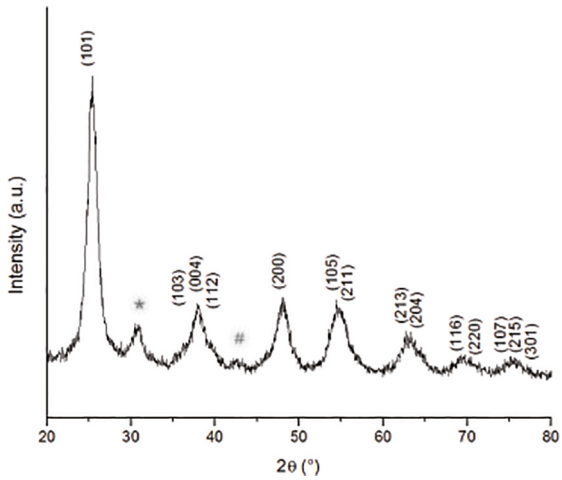

Figure 1: Typical XRD patterns of TiO_2 nanoparticles synthesized in acidic conditions, in this case the for the sample HM110-5min.

The crystallites size was estimated using the Scherrer equation[30] and it was found to be close to 6.0 nm for all materials analysed; for this purpose the most intense peak at 2θ = 25.49 º was used, see Table S2 in the Supplementary Material. The intensity of the diffraction peak is correlated to the volume of the phase and crystallite size. For very small crystallites, the peaks are broad as can be seen in Figure 1.

No clear dependence on the particle size or its morphology was observed according with the synthesis parameters used, as observed in SEM and TEM images, Figure 2 and 3. Analyzing the images, it is possible to note that the particles are agglomerated. Aggregation is expected due to the presence of a $Ti(OH)_n$ amorphous phase, due to the lack of a sintering step. In Figure 2, SEM images of HM110-15 and HM150-60 are presented, for other samples see Figure S2 in the Supplementary Material.

On the order hand, analyzing the TEM images, Figure 3a and 3b, it is possible to observe that the nanoparticles have sizes between 10 and 15 nm (sample HM150-30), which was confirmed from the size distribution study, made using ImageJ sotware presented in Figure S3. The Selected Area

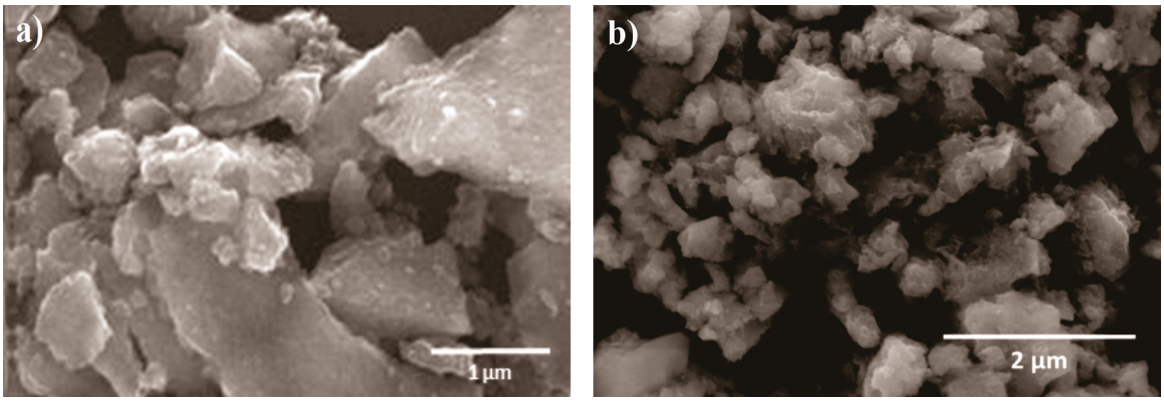

Figure 2: SEM images of samples prepared at a) HM110-15 and, b) HM150-60.

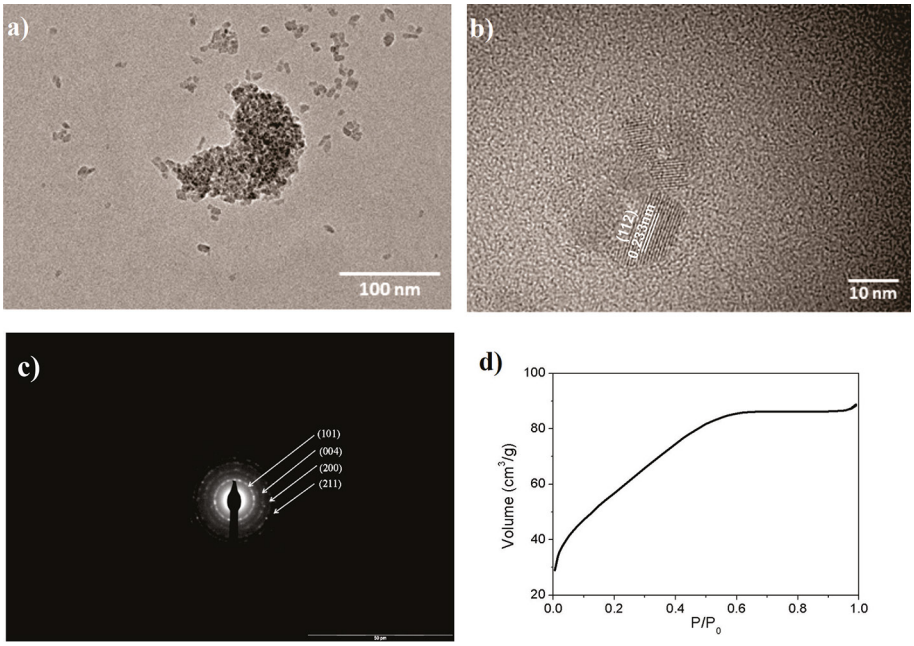

Figure 3: TEM images obtained with different magnifications (a) and (b), Electron Diffraction Pattern (c) and BET adsorption curve (d) for sample HM150-30.

Electron Diffraction Pattern (SAED) in Figure 3c shows in agreement with the X-ray diffraction that the samples are predominantly crystalline. The surface area from BET for this sample is 207 m^2/g. The adsorption curve shown in Figure 3d is typical for a microporous material with relatively small external surface.[31]

In summary, the synthesis parameter used do not affect the morphology, crystallite size and crystalline phase however, they do influence the nanoparticles synthesis yield. For short times, 2 and 5 minutes, the yield obtained were lower than 30% even at the highest temperature. Whereas the synthesis yields at 150 °C and 30 min was 93%. For the yield determination, each reaction was repeated at least 3 times and the yields presented in Table S1 are the average values fond.

The best yields were obtained for synthesis from 30 to 60 min at 150 °C. In order to understand the different yields observed and the small dependence of the nanoparticles obtained on synthesis parameters, we shall start discussing the nanoparticles synthesis reaction. The precursor solution is formed with the loss of the organic groups from TTIP and hydrolysis, which leds to the formation of $Ti(OH)_x(OCHCH_3)_{4-x}$ species. The hydrolysis reaction of titanium alkoxide is a fast process and dominates the morphology and final particle size, for that reason the precursor solution was slowly dropped into water and kept under vigourous stirring at 80 °C when a whitish transparent solution was obtained. In the second step, the addition of HNO_3 acts as a peptizing agent forming crystallites with low crystallinity by hydrolysis.[3] In aqueous medium, protonated surfaces of TiO_6 octahedra easily combine with hydroxyl groups of other TiO_6 octahedra to form Ti–O–Ti bonds by water elimination,[14] resulting in amorphous nanoparticles.[34,35] The use of microwave hydrothermal

processing of colloidal TiO_2 solutions allows rapid heating, fast kinetics of crystallization and formation of a large number of clusters that grows from amorphous nanoparticles and assemble into TiO_2 nanocrystallite aggregates.[36] This reaction is characterized by the formation of a high concentration of aggregated nanoparticles. Additionally, it is known that the size of the particle and additional conditions such as surface stress/strain influence the crystalline phase.[37-39] In general, anatase is the most stable crystalline phase for particles smaller than 11 nm, brookite for particles between 11 and 35 nm and rutile for particles bigger than 35 nm.[40] In this way, our results indicate that the fast cluster formation, due to the microwave heating, is responsible for the small crystallites and nanoparticles obtained as well as its aggregation. The crystalline materials formed exhibits the predominance of the anatase phase with some brookite nanoparticles formed due to the pressures inside the autoclave. Normally the simplest way to control the crystal size is by microwave synthesis time. However, in our results there is no clear difference in the size of the nanoparticles depending on time. The crystal growth mechanism observed is compatible to an oriented aggregation of small primary subunits.[41] We observed the highest yields for the highest temperature and times higher than 30 min. Thus, it is assumed that in this system, 30 min is the minimum synthesis time for the nucleation and growth of the nanoparticles. For times higher than 30 min no difference in yield is observed which can be attributed to the Ostwald ripening process, in which the particles re-dissolve after a critical time, thus the yield is basically time independent after this time.[42] Notice that in microwave hydrothermal synthesis high internal surface areas are expected,[43] in our case 207 m^2/g.

3.2 Alkaline medium

Similarly, the syntheses under alkaline environments were performed in different conditions. The temperature was 110, 130 and 150 °C, using 5, 15, 30 and 60 min of treatment time for the concentration of 1 and 10 M

We shall start with the effect of the synthesis time in the 1M precursor solution. The XRD patterns for these samples are presented in Figure 4 (see also Figure S4 for 110, 130 and 150 °C). The diffraction patterns are similar for all the synthetic conditions. They have shown a preferred orientation in the direction of the peak at $2\theta = 48.1$ ° which can be attributed to $Na_2Ti_6O_{13}$ (JCPDS 73-1398).[32] Analogous to the acidic system, the synthesis time did not influence the crystalline phase and morphology. However, the time influences the yield of the synthesis and the optimum yield, > 90 %, was obtained after 30 min of synthesis.

The influence of Na^+ in the crystal growth was addressed using different NaOH concentrations during the synthesis. In Figure 5 the XRD patterns for the powders prepared using 10 M (HMB150-30-10) and 0.1 M (HMB150-30-0.1)

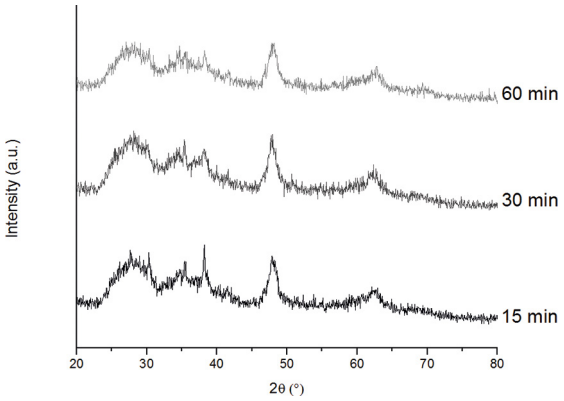

Figure 4: XRD patterns for the syntheses material using 1 M NaOH at 150 ° C, using different times 15, 30 and 60 min.

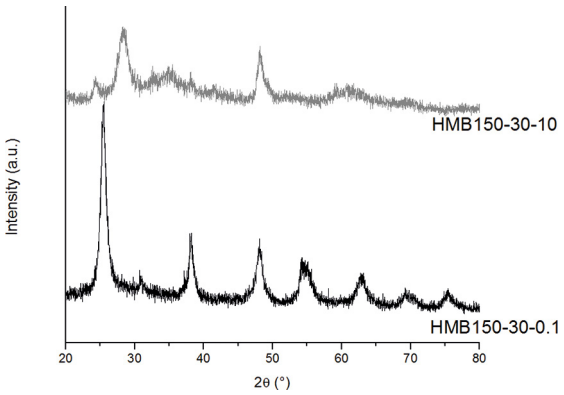

Figure 5: XRD patterns for the samples HMB150-30-10 and HMB150-30-0.1.

are shown. It can be seen that the sample with the highest concentration of NaOH follows the same diffraction pattern of the titanates, in this case $Na_2Ti_3O_7$ (JCPDS 31-1329).[33] The lower concentration shows the anatase phase, similarly to Figure 1. Notice that the peak of the brookite phase in $2\theta = 31°$ is observed for the sample HMB150-30-0.1.

From SEM images, Figure 6, it was possible to observe that the samples with low concentration of NaOH and the samples synthesized in acidic medium (Figure 2 and 6a) present similar morphology and the samples synthetized using 10 M NaOH (Figure 6b) present morphology dominated by needle-like structures. The SEM image of the samples HMB150-30-1(Figure 6c) presents a mixture of needle like structures and irregular spheres as observed in lower concentrations of NaOH.

The BET adsorption curve, Figure 6d, shows a steep increase in the isotherm, followed by a plateau which indicates a microporous material with relatively small external surface. The plateau is reached as soon as the surface is completely covered.[31] Due the difference on the morphology of the nanoparticles synthetized in acid and alkaline medium, the surface area value of the sample HMB150-30-10 obtained by BET is high, 375 m^2/g.

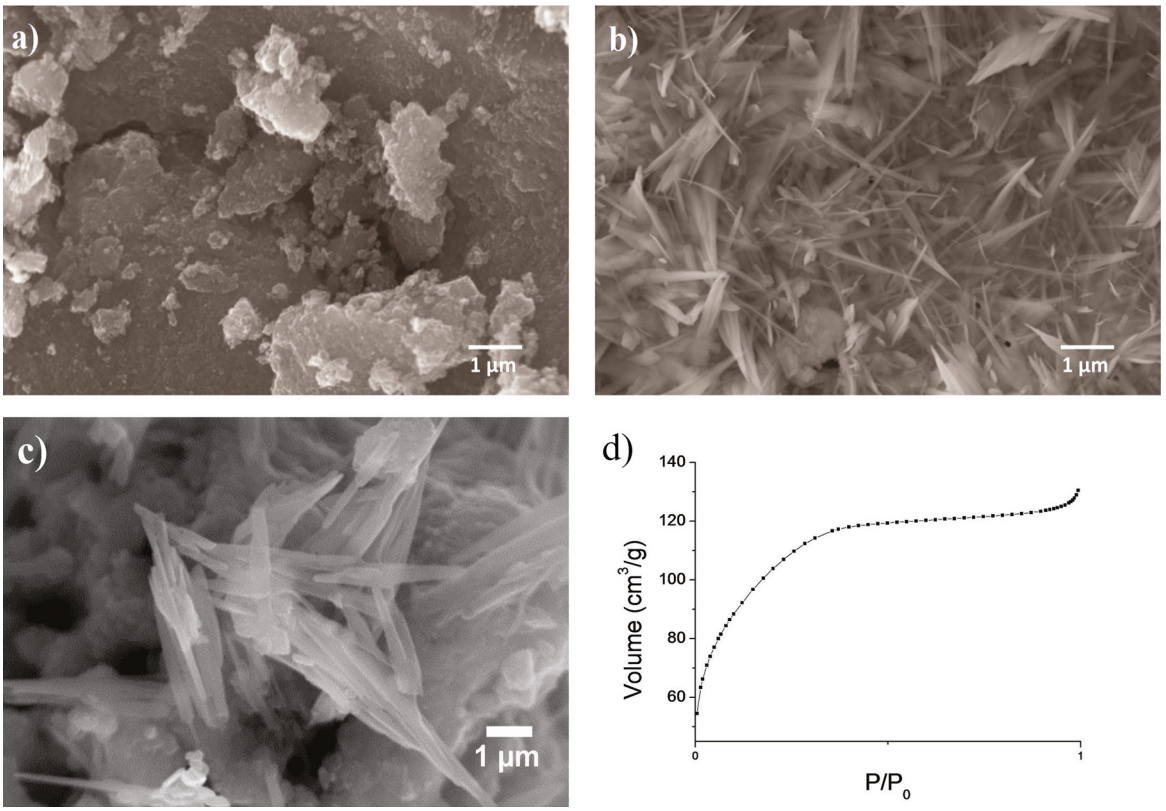

Figure 6: SEM images for the samples a) HMB150-30-0.1, b) HMB150-30-10, c) HMB150-30-1 and d) HMB150-30-10 BET adsorption curve.

The SEM images of the samples synthesized at 110 °C present sphere-like aggregated that are composed by nanosheets, observed in higher magnifications, Figure S6a and Figure S6b. The samples synthesized at 130 °C presented a mixture of nanocables and nanoparticles, and the same trend of nanosheets observed in lower temperature of treatment, Figure S6c, Figure S6d and Figure S6e. The sample synthesized at 150 °C present a mixture of needle like structures and irregular spheres as observed in lower concentrations of NaOH, Figure S6f, Figure S6g and Figure S6h. It is important to note that the same trend of morphologies were observed in the various temperatures, however, the samples treated at 5 min, presented the most heterogeneous and bigger nanoparticles, Figure S6g.

TEM image of the sample HMB150-30-10 after HCl washing is shown in Figure 7a. It is possible to observe aggregated nanotube-like structures. Na^+ ions are detected by EDX in both samples, as synthetized and after washing, as presented in Figure 7b and 7c. However, the sample after washing, Figure 7c, has the peak attributed to Na^+ ions decreased to 0.2 of initial value, suggesting that the Na^+ ions are removed by HCl washing. The peaks of Si are coming from the substrate used for the EDX measurements.

In the hydrothermal synthesis the morphology and phase formation are more related with the pressure and temperature inside the reactor[45] during the polycondensation step. The TiO_2 formation is weakly affected by the additive, HNO_3 or NaOH when it is close to the neutral condition, i.e. 0.01 M HNO_3 and 0.1 M NaOH,[46] which explains the higher crystallinity for HMB150-30-0.1 compared to HMB150-30-10. On the other hand, at high NaOH concentrations, 1 M and 10 M, remarkable differences were observed, needle-like titanates were synthesized, probably due to the influence of Na^+ ions on the formation of the crystalline structure.

In the literature few works are dedicated to investigate the influence of acidic and alkaline environments using TTIP as precursor on the nanoparticles formation. Zhao et al.[46] have study the influence of the NaOH and HCl on the formation of nanostructures with different crystalline phase and morphologies using hydrothermal synthesis and tetrabutyl titanate as precursor. They obtained analogous materials as we did, i.e. anatase with brookite for the lowest concentrations of additives, or in conditions closest to neutral. For high NaOH concentrations, they obtained titanate nanoribbons. The difference between our material morphology and theirs can be attributed to the precursor used and synthesis technique. The ability of microwaves to influence the dissolution rate of various precursors (due to different dielectric properties) strongly affects the nucleation and crystallization rates. The organic species undergo chemical

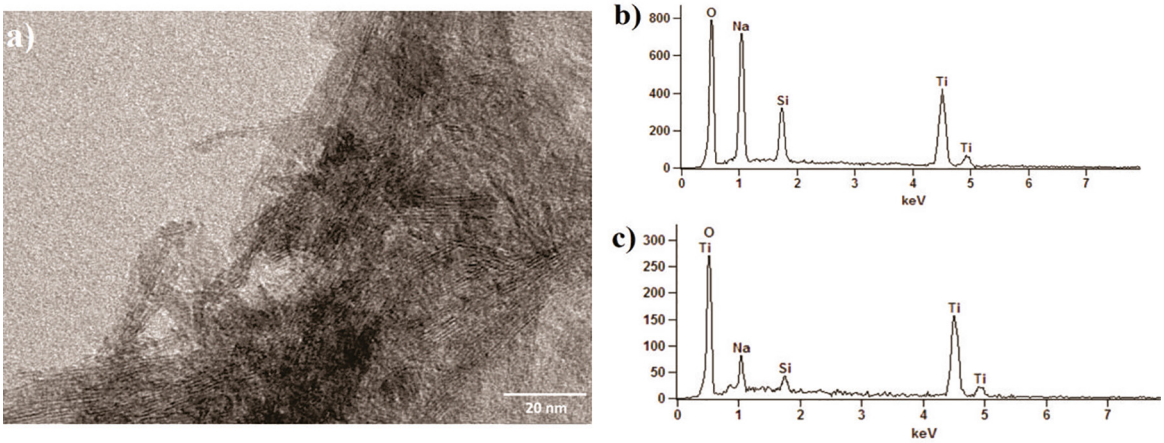

Figure 7: a) TEM image and b) EDX for the sample HMB150-30-10 as synthetized and c) EDX for the sample HMB150-30-10 after HCl washing.

reactions that are responsible for supplying the ''monomers'' for nucleation and growth of the inorganic nanoparticles,[47] which can be related to the pronounced shape anisotropy observed in Figure 5. In this way, the reaction proposed for the formation of the needle-like structures is based on the most accepted mechanism for nanotubes formation starting from TiO_2 spherical nanoparticles. Ti – O –Ti bonds are broken by NaOH to create an intermediate containing Ti – O – Na and Ti – OH bonds,[9] which grows in preferential directions. Instead, in our case the hydrolyses of TTIP directly on the solution forms intermediates that have the format of sheets due to the interaction of the TiO layers with Na^+ and H^+. The growth generates layered titanate structure with intercalated Na^+ ions.[46] As shown in Figure 7b and 7c, some of the Na^+ ions can be removed by HCl rinsing.[13] Here, we have obtained aggregated nanotube-like structures in 30 min of treatment using TTIP as precursor with high surface areas, of 375 m^2/g.

From the point of view of applications, Dar et al.[5] obtained anatase nanostructures ~ 7 nm using microwave solvothermal technique using titanium thiobenzoate complexes as precursor at 200 °C and fabricated from this materials DSSC with efficiencies of 6.5%. Shen and coworkers, used also TTIP as precursor, and did their synthesis at 220 °C for 30 min. They obtained anatase nanoparticles with ~ 20 nm in diameter and surface area of 152 m^2/g which were used in DSSC with conversion efficiency of 7.8%.[25] Thus our results indicate that the synthesized nanoparticles with up to 375 m^2/g of surface area have great potential in DSSC.

4. Conclusions

Nanostructured titanium oxide was successfully synthesized by the microwave assisted hydrothermal technique. The nanoparticles were obtained at mild conditions using low temperatures and short synthesis times, as low as 2 minutes. The XRD patterns show that the TiO_2 nanocrystals are predominantly in the anatase crystal phase though brookite crystalites are also present. The crystallite sizes in acidic solutions have 5 to 6 nm in diameter and aggregate into particles of 15 nm. The reaction time and temperature do not change significantly the structure of the material. In the presence of high concentration of NaOH the morphology and phase are changed to titanates nanotube-like structures, obtained after 30 min of synthesis. The structures obtained, that resemble needles, have the crystalline phase of $Na_2Ti_6O_{13}$ and $Na_2Ti_3O_7$. For lower NaOH concentrations aggregated nanoparticles were obtained similar to the ones obtained using HNO_3 as peptizing agent. In both systems, high surface areas were obtained which indicates that these materials are suited for photovoltaics or catalysis.

5. Acknowledgements

The authors would like to thank the financial support of FAPESP (2011/02205-3), CEPID-FAPESP (2013/07296-2), INCT, CNPq and CAPES.

6. References

1. Chen X, Mao SS. Titanium Dioxide Nanomaterials: Synthesis, Properties, Modifications, and Applications. *Chemical Reviews*. 2007;107(7):2891-2959. DOI: 10.1021/cr0500535.

2. Chen D, Huang F, Cheng YB, Caruso RA. Mesoporous Anatase TiO_2 Beads with High Surface Areas and Controllable Pore Sizes: A Superior Candidate for High-Performance Dye-Sensitized Solar Cells. *Advanced Materials*. 2009;21(21):2206-2210. DOI: 10.1002/adma.200802603.

3. Ismail AA, Bahnemann DW. Mesoporous titania photocatalysts: preparation, characterization and reaction mechanisms. *Journal of Materials Chemistry.* 2011;21(32):11686-11707. DOI: 10.1039/C1JM10407A.

4. Tang H, Lévy F, Berger H, Schmid PE. Urbach tail of anatase TiO_2. *Physical Review B*. 1995;52 (11):7771-7774.

5. Dar MI, Chandiran AK, Grätzel M, Nazeeruddin MK, Shivashankar SA. Controlled synthesis of TiO_2 nanoparticles and nanospheres using a microwave assisted approach for their application in dye-sensitized solar cells. *Journal of Materials Chemistry A*. 2014;2(6):1662-1667. DOI: 10.1039/C3TA14130F.

6. Mbonyiryivuze A, Zongo S, Diallo A, Bertrand S, Minani E, Yadav LL, et al. Titanium Dioxide Nanoparticles Biosynthesis for Dye Sensitized Solar Cells application: Review. *Physics and Materials Chemistry*. 2015;3(1):12-17. DOI: 10.12691/pmc-3-1-3.

7. Melcarne G, De Marco L, Carlino E, Martina F, Manca M, Cingolani R, et al. Surfactant-free synthesis of pure anatase TiO_2 nanorods suitable for dye-sensitized solar cells. *Journal of Materials Chemistry*. 2010;20(34):7248-7254. DOI: 10.1039/C0JM01167C.

8. Bavykin DV, Friedrich JM, Walsh FC. Protonated Titanates and TiO_2 Nanostructured Materials: Synthesis, Properties, and Applications. *Advanced Materials*. 2016;18(21):2807-2824. DOI: 10.1002/adma.200502696.

9. Liu N, Chen X, Zhang J, Schwank JW. A review on TiO_2-based nanotubes synthesized via hydrothermal method: Formation mechanism, structure modification, and photocatalytic applications. *Catalysis Today*. 2014;225:34-51. DOI: 10.1016/j.cattod.2013.10.090.

10. Ou HH, Lo SL. Review of titania nanotubes synthesized via the hydrothermal treatment: Fabrication, modification, and application. *Separation and Purification Technology*. 2007;58(1):179-191. DOI: 10.1016/j.seppur.2007.07.017.

11. Mao Y, Park TJ, Zhang F, Zhou H, Wong SS. Environmentally Friendly Methodologies of Nanostructure Synthesis. *Small*. 2007;3(7):1122-1139. DOI: 10.1002/smll.200700048.

12. Kim DS, Kwak SY. The hydrothermal synthesis of mesoporous TiO_2 with high crystallinity, thermal stability, large surface area, and enhanced photocatalytic activity. *Applied Catalysis A: General*. 2007;323:110-118. DOI: 10.1016/j.apcata.2007.02.010.

13. Kasuga T, Hiramatsu M, Hoson A, Sekino T, Niihara K. Formation of Titanium Oxide Nanotube. *Langmuir*. 1998;14(12):3160-3163. DOI: 10.1021/la9713816.

14. Jiang B, Yin H, Jiang T, Jiang Y, Feng H, Chen K, et al. Hydrothermal synthesis of rutile TiO_2 nanoparticles using hydroxyl and carboxyl group-containing organics as modifiers. *Materials Chemistry and Physics*. 2006;98(2-3):231-235. DOI: 10.1016/j.matchemphys.2005.09.044.

15. Nakahira A, Kubo T, Numako C. Formation Mechanism of TiO_2-Derived Titanate Nanotubes Prepared by the Hydrothermal Process. *Inorganic Chemistry*. 2010;49(13):5845-5852. DOI: 10.1021/ic9025816.

16. Corradi AB, Bondioli F, Focher B, Ferrari AM, Grippo C, Mariani E, et al. Conventional and Microwave-Hydrothermal Synthesis of TiO_2 Nanopowders. *Journal of the American Ceramic Society*. 2005;88(9):2639-2641. DOI: 10.1111/j.1551-2916.2005.00474.x.

17. Kumar R, Singh RK, Vaz AR, Moshkalev SA. Microwave-assisted synthesis and deposition of a thin ZnO layer on microwave-exfoliated graphene: optical and electrochemical evaluations. *RSC Advances*. 2015;5(83):67988-67995. DOI: 10.1039/C5RA09936F.

18. Kumar R, Singh RK, Singh DP, Savu R, Moshkalev SA. Microwave heating time dependent synthesis of various dimensional graphene oxide supported hierarchical ZnO nanostructures and its photoluminescence studies. *Materials & Design*. 2016;111:291-300. DOI: 10.1016/j.matdes.2016.09.018.

19. Kumar R, Singh RK, Savu R, Dubey PK, Kumar P, Moshkalev SA. Microwave-assisted synthesis of void-induced graphene-wrapped nickel oxide hybrids for supercapacitor applications. *RSC Advances*. 2016;6(32):26612-26620. DOI: 10.1039/C6RA00426A.

20. Kumar R, Singh RK, Dubey PK, Singh DP, Yadav RM. Self-Assembled Hierarchical Formation of Conjugated 3D Cobalt Oxide Nanobead–CNT–Graphene Nanostructure Using Microwaves for High-Performance Supercapacitor Electrode. *ACS Applied Materials & Interfaces*. 2015;7(27):15042-15051. DOI: 10.1021/acsami.5b04336.

21.Kumar R, Dubey PK, Singh RK, Vaz AR, Moshkalev SA. Catalyst-free synthesis of a three-dimensional nanoworm-like gallium oxide–graphene nanosheet hybrid structure with enhanced optical properties. *RSC Advances*. 2016;6(21):17669-17677. DOI: 10.1039/C5RA24577J.

22. Manfroi DC, dos Anjos A, Cavalheiro AA, Perazolli LA, Varela JA, Zaghete MA. Titanate nanotubes produced from microwave-assisted hydrothermal synthesis: Photocatalytic and structural properties. *Ceramics International*. 2014;40(9 Pt A):14483-14491. DOI: 10.1016/j.ceramint.2014.07.007.

23. Cui L, Hui KN, Hui KS, Lee SK, Zhou W, Wan ZP, et al. Facile microwave-assisted hydrothermal synthesis of TiO_2 nanotubes. *Materials Letters*. 2012;75:175-178. DOI: 10.1016/j.matlet.2012.02.004.

24. Wu X, Jiang QZ, Ma ZF, Fu M, Shangguan WF. Synthesis of titania nanotubes by microwave irradiation. *Solid State Communications*. 2005;136(9-10):513-517. DOI: 10.1016/j.ssc.2005.09.023.

25. Shen PS, Tai YC, Chen P, Wu YC. Clean and time-effective synthesis of anatase TiO_2 nanocrystalline by microwave-assisted solvothermal method for dye-sensitized solar cells. *Journal of Power Sources*. 2014;247:444-451. DOI: 10.1016/j.jpowsour.2013.08.104.

26. Pang YL, Lim S, Ong HC, Chong WT. A critical review on the recent progress of synthesizing techniques and fabrication of TiO_2-based nanotubes photocatalysts. *Applied Catalysis A: General*. 2014;481:127-142. DOI: 10.1016/j.apcata.2014.05.007.

27. Saponjic ZV, Dimitrijevic NM, Tiede DM, Goshe AJ, Zuo X, Chen LX, et al. Shaping Nanometer-Scale Architecture Through Surface Chemistry. *Advanced Materials*. 2005;17(8):965-971. DOI: 10.1002/adma.200401041.

28. Di Paola A, Bellardita M, Palmisano L. Brookite, the Least Known TiO_2 Photocatalyst. *Catalysts*. 2013;3(1):36-73. DOI: 10.3390/catal3010036.

29. Kumar R, Singh RK, Dubey PK, Singh DP, Yadav RM, Tiwari RS. Hydrothermal synthesis of a uniformly dispersed hybrid graphene–TiO_2 nanostructure for optical and enhanced electrochemical applications. *RSC Advances*. 2015;5(10):7112-7120. DOI: 10.1039/C4RA06852A.

30. Patterson AL. The Scherrer Formula for X-Ray Particle Size Determination. *Physical Review*. 1939;56(10):978.

31. Sing KSW. Reporting Physisorption Data for Gas/Solid Systems with Special Reference to the Determination of Surface Area and Porosity (Recommendations 1984). *Pure and Applied Chemistry*. 1985;57(4):603-619.

32. Andersson S, Wadsley AD. The structures of $Na_2Ti_6O_{13}$ and $Rb_2Ti_6O_{13}$ and the alkali metal titanates. *Acta Crystallographica*. 1962;15:194-201. DOI: 10.1107/S0365110X62000511.

33. Yang J, Li D, Wang X, Yang X, Lu L. Study on the synthesis and ion-exchange properties of layered titanate $Na_2Ti_3O_7$ powders with different sizes. *Journal of Materials Science*. 2003;38(13):2907-2911. DOI: 10.1023/a:1024401006582.

34. Brinker CJ. Hydrolysis and condensation of silicates: Effects on structure. *Journal of Non-Crystalline Solids*. 1988;100(1-3):31-50. DOI: 10.1016/0022-3093(88)90005-1.

35. Yin H, Wada Y, Kitamura T, Kambe S, Murasawa S, Mori H, et al. Hydrothermal synthesis of nanosized anatase and rutile TiO_2 using amorphous phase TiO_2. *Journal of Materials Chemistry*. 2001;11(6):1694-1703. DOI: 10.1039/B008974p.

36. Wilson GJ, Will GD, Frost RL, Montgomery SA. Efficient microwave hydrothermal preparation of nanocrystalline anatase TiO_2 colloids. *Journal of Materials Chemistry*. 2002;12(6):1787-1791. DOI: 10.1039/B200053A.

37. Hearne GR, Zhao J, Dawe AM, Pischedda V, Maaza M, Nieuwoudt MK, et al. Effect of grain size on structural transitions in anatase TiO_2: A Raman spectroscopy study at high pressure. *Physical Review B*. 2004;70:134102.

38. Hazem R, Izerrouken M, Sari A, Kermadi S, Msimanga M, Benyagoub A, et al. Radiation damage induced by swift heavy ions in TiO_2 sol–gel films nanocrystallines. *Nuclear Instruments and Methods in Physics Research Section B: Beam Interactions with Materials and Atoms*. 2013;304:16-22. DOI: 10.1016/j.nimb.2013.03.037.

39. Franklyn PJ, Levendis DC, Coville NJ, Maaza M. Phase Transformation of Hydrothermally Synthesized Nanoparticle TiO_2: from Anatase to Rutile Nanorods. *South African Journal of Chemistry*. 2007;60(1):71-75.

40. Zhang H, Banfield JF. Understanding Polymorphic Phase Transformation Behavior during Growth of Nanocrystalline Aggregates: Insights from TiO_2. *The Journal of Physical Chemistry B*. 2000;104(15):3481-3487. DOI: 10.1021/jp000499j.

41. Luo L, Hui J, Yu Q, Zhang Z, Jing D, Wang P, et al. Crystal growth by leaps and bounds based on self-assembly: insight from titania. *CrystEngComm*. 2012;14(22):7648-7655. DOI: 10.1039/C2CE25812A.

42. Wilson GJ, Matijasevich AS, Mitchell DRG, Schulz JC, Will GD. Modification of TiO_2 for Enhanced Surface Properties: Finite Ostwald Ripening by a Microwave Hydrothermal Process. *Langmuir*. 2006;22(5):2016-2027. DOI: 10.1021/la052716j.

43. Chen P, Peng JD, Liao CH, Shen PS, Kuo PL. Microwave-assisted hydrothermal synthesis of TiO spheres with efficient photovoltaic performance for dye-sensitized solar cells. *Journal of Nanoparticle Research*. 2013;15:1465. DOI: 10.1007/s11051-013-1465-0.

44. Bacsa RR, Grätzel M. Rutile Formation in Hydrothermally Crystallized Nanosized Titania. *Journal of the American Ceramic Society*. 1996;79(8):2185-2188. DOI: 10.1111/j.1151-2916.1996.tb08956.x.

45. Aruna ST, Tirosh S, Zaban A. Nanosize rutile titania particle synthesis *via* a hydrothermal method without mineralizers. *Journal of Materials Chemistry*. 2000;10(10):2388-2391. DOI: 10.1039/B001718N.

46. Zhao B, Lin L, He D. Phase and morphological transitions of titania/titanate nanostructures from an acid to an alkali hydrothermal environment. *Journal of Materials Chemistry A*. 2013;1(5):1659-1668. DOI: 10.1039/C2TA00755J.

47. Bilecka I, Niederberger M . Microwave chemistry for inorganic nanomaterials synthesis. *Nanoscale*. 2010;2(8):1358-1374. DOI: 10.1039/B9NR00377K.

Supplementary material

The following online material is available for this article:

Structural information of the surfaces